


Imaging Advances in Heart Failure

Ritu Thamman ¹, Naeimeh Hosseini ², Marie-Luise Dikou ², Imtiaz U Hassan ², Oksana Marchenko ²,
Olukayode Abiola ³ and Julia Grapsa ²

1. Department of Cardiology, University of Pittsburgh School of Medicine, Pittsburgh, PA, US; 2. Department of Cardiology, St Thomas' Hospital, London, UK; 3. Department of Cardiology, Lister General Hospital, Stevenage, Hertfordshire, UK

Abstract

This paper delves into the significance of imaging in the diagnosis, aetiology and therapeutic guidance of heart failure, aiming to facilitate early referral and improve patient outcomes. Imaging plays a crucial role not only in assessing left ventricular ejection fraction, but also in characterising the underlying cardiac abnormalities and reaching a specific diagnosis. By providing valuable data on cardiac structure, function and haemodynamics, imaging helps diagnose the condition, evaluate haemodynamic status and, consequently, identify the underlying pathophysiological phenotype, as well as stratifying the risk for outcomes. In this article, we provide a comprehensive exploration of these aspects.

Keywords

Imaging, congestive heart failure, heart failure with preserved ejection fraction, heart failure with reduced ejection fraction

Received: 10 May 2023 **Accepted:** 17 October 2023 **Citation:** *Cardiac Failure Review* 2024;10:e12. **DOI:** <https://doi.org/10.15420/cfr.2023.10>

Disclosure: JG is on the *Cardiac Failure Review* editorial board; this did not influence peer review. All other authors have no conflicts of interest to declare.

Correspondence: Ritu Thamman, Department of Cardiology, University of Pittsburgh School of Medicine, 490 E North Ave, Suite G104, Pittsburgh, PA 15212, US. E: thammanr2@upmc.edu

Copyright: © The Author(s) 2024. This work is open access and is licensed under CC BY-NC 4.0. Users may copy, redistribute and make derivative works for non-commercial purposes, provided the original work is cited correctly.

Imaging is indispensable for the diagnosis of heart failure (HF), determining its aetiology, and for therapeutic guidance, with the goal of early referral and better patient outcomes. HF with preserved ejection fraction (HFpEF) is a syndrome defined by a left ventricular ejection fraction (LVEF) >50%, whereas HF with reduced ejection fraction (HFrEF) is defined by an LVEF <40%.¹

Although the prevalence rate of HFrEF has declined over the past few decades, the prevalence of HFpEF has risen, now accounting for more than 50% of all HF cases.²

The number of patients with HF has been increasing due to the ageing population, global population growth and improved survival after diagnosis.³

Distinct underlying cellular and molecular mechanisms between HFrEF and HFpEF account for the differences seen on imaging. Although HF is a clinical diagnosis, imaging is key to its correct diagnosis. Imaging is key not only in measuring LVEF, but also in characterising the underlying cardiac pathology and arriving at a specific diagnosis. Imaging data on cardiac structure, function and haemodynamics provide a diagnosis and evaluate haemodynamic status, thus helping determine the underlying pathophysiological phenotype and to risk stratify for outcomes. This paper elaborates on these issues (*Figure 1*).

Definitions of Heart Failure

Based on LVEF, there are now four categories of HF: HFrEF (LVEF <40%); HF with mildly reduced ejection fraction (HFmrEF; LVEF 41–49%); HFpEF (LVEF >50%); and, finally, HF with improved ejection fraction (HFimpEF).

HFimpEF is defined as patients with baseline LVEF <40% but with an at least 10-point improvement in LVEF from baseline, with the second measurement (performed between 1 month and 1 year after discharge) being >40%. This characterisation is important to avail evidence-based treatments for these different categories.⁴

A substantial proportion of older adults with HFpEF in the community are likely to be undiagnosed, especially black individuals, who have lower natriuretic peptide concentrations than white individuals.⁵ A recent study on the spectrum of HFpEF phenotypes found that in patients with unexplained exertional dyspnoea, using an algorithmic H₂FPEF score led to less misclassification and improved diagnostic accuracy compared with the conventional approach of exercise pulmonary artery capillary wedge pressures, divided into three groups: one with exercise-induced left atrial (LA) hypertension, one with resting LA hypertension and one with overt right ventricle (RV) failure.⁶

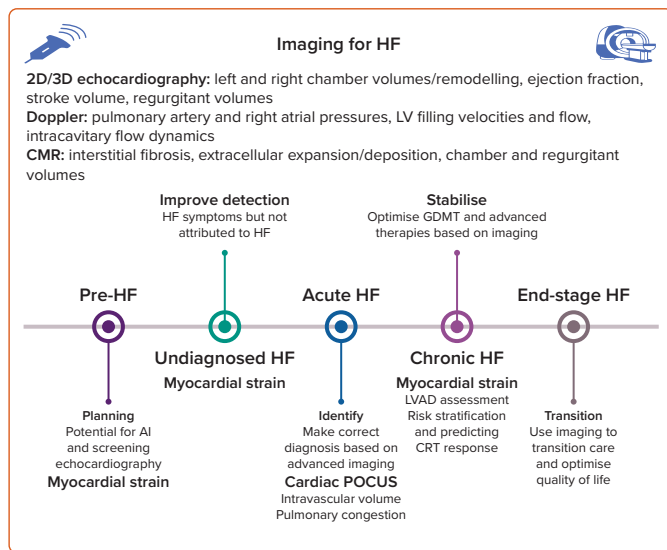
In the analysis from the ARIC study, black patients made up a larger proportion of those with undiagnosed dyspnoea (20.7% of patients in the lowest score category and 38.3% in the highest risk category were black; $p < 0.001$).⁷ Given sodium–glucose cotransporter 2 inhibitors are an effective treatment, awareness and recognition of HFpEF is key to curtailing the rising numbers of cases of HFpEF.⁸

Imaging Assessments

3D Left Ventricular Volume/Chamber Size

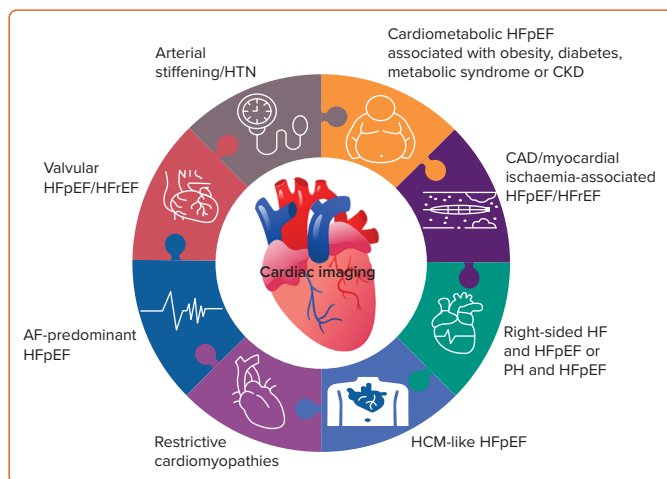
Imaging can characterise chamber size in patients with HF, which is key for diagnosis (*Figure 2*). Echocardiography is the most common

Figure 1: Overview of Imaging for Congestive Heart Failure



AI = artificial intelligence; CMR = cardiac MRI; GDMT = guideline-directed medical therapy; HF = heart failure; LV = left ventricle; LVAD = left ventricular assist device; POCUS = point of care ultrasound.

Figure 2: Heart Failure is Clinically Heterogeneous



CAD = coronary artery disease; CKD = chronic kidney disease; HCM = hypertrophic cardiomyopathy; HF = heart failure; HFpEF = heart failure with preserved ejection fraction; HFrEF = heart failure with reduced ejection fraction; HTN = hypertension; PH = pulmonary hypertension.

non-invasive imaging modality used to quantify cardiac chamber size and function due to its widespread availability, portability and the ability of real-time imaging without any extraordinary contraindications.

If need be, echocardiography can be augmented by other imaging modalities, such as cardiac MRI (CMR) in case of a difficult imaging window or borderline cases.

Most commonly, left ventricular (LV) volume and subsequent ejection fraction are obtained by 2D echocardiography by endocardial tracings using the biplane method of disks. However, LV views must not have apical foreshortening and have adequate visualisation of all segments in the apical four-chamber view.

LV cavity size is mostly assessed by measuring linear internal dimensions at end-diastole and end-systole in the parasternal long-axis view and reported as indexed to body surface area. LV volume is measured from

apical two- and four-chamber views, measuring maximum LV area by avoiding foreshortening, which can be avoided by acquisition at a reduced depth to focus on LV cavity.⁹

Similarly, RV size is assessed by linear measurements in RV-focused views at end-diastole, such as RVD1 (defined as the maximum transverse diameter in the basal one-third), RVD2 (defined as the diameter at the middle one-third of the RV inflow) and the maximum longitudinal measurement from the mid-point of the RV annular plane to the RV apex. RV function can be assessed by different methods in 2D using colour and tissue Doppler. RV fractional area change on echocardiography yields results comparable to CMR. Longitudinal function is mostly assessed by tricuspid annular plane systolic excursion (TAPSE) and RV peak lateral tricuspid annular systolic velocity (S'), which is obtained by pulsed-wave tissue Doppler imaging, and is simple and reproducible, with established prognostic value.⁹

However, 3D volumes are more reproducible and correlate with CMR-derived volumes better than 2D volumes.¹⁰ Compared with 2D assessment, 3D echocardiography (3DE) has emerged as the most accurate, reliable and reproducible echocardiographic technique for LV quantification, with less interoperator variability and a lack of reliance on geometric assumptions.¹¹

3DE has consistently demonstrated good accuracy and reproducibility in a time-saving manner for the evaluation of LV volumes and LVEF in validation studies against the presumed gold standard CMR.¹² 3DE slightly underestimates LV quantification compared with CMR due to compromised spatial resolution and different methods of endocardial border delineation. However, with increasing operator experience and improved uniformity of the quantification method, there is increasingly improved agreement between 3DE and CMR volume assessment.^{13,14}

Ultrasound Enhancing Agents

Ultrasound enhancing agents (UEAs) are microbubbles that enhance ultrasound signals. LV volumes obtained with UEAs are typically larger than those measured without UEAs. Although the normal range for LVEF does not appear to be different, new reference ranges for end-diastolic and end-systolic LV volumes when using UEAs should be established.¹⁵

Disease-specific Imaging Pulmonary Hypertension

Both systolic and diastolic HF cause pulmonary hypertension, due, in part, to raised pulmonary venous pressure and, in part, to vascular remodelling. There is a vast array of aetiologies for HF-related pulmonary hypertension, ranging from congenital heart disease to the left-sided heart pathologies to systemic diseases like systemic lupus erythematosus. Eighty per cent of patients with HFpEF have pulmonary hypertension, some just from elevated LA pressures, and in some patients pulmonary hypertension leads to pulmonary vascular disease.¹⁶

The RV initially adapts to increased afterload by increasing the force of contraction, but later fails, causing uncoupling of the RV and pulmonary circulation, ending up with dilated RV and systemic congestion.¹⁷

Both 2D and 3D parameters for RV function assessment have been used effectively, but combining these measurements with pulmonary arterial pressures has proven to be prognostically more significant and provides a true reflection of RV–pulmonary artery (PA) coupling. Ventriculoarterial coupling refers to the relationship between ventricular contractility and

afterload. Its most objective metric is the ratio between ventricular elastance as a measure of contractility and arterial elastance as a measure of afterload. As RV wall stress increases, the RV wall thickness increases before RV dilation is observed. These changes can be measured using standard metrics.¹⁸ One such measure, the non-invasively measured TAPSE/systolic PA pressure (PAP) ratio on echocardiography, has been proven to predict event-free survival, with a cut-off <0.35 mm/mmHg consistent with poor prognosis.¹⁷

Patients with discordance of echocardiographic parameters presented with significantly higher New York Heart Association (NYHA) class, worse functional capacity, higher invasive right atrial pressure, worse LV function, the lowest echocardiographic systolic PAP measurements and more severe tricuspid regurgitation (TR). Echocardiographic predictors of discordance included LVEF $<50\%$, TAPSE <17 mm, V-wave cut-off sign (triangular spectral profile) and TR Grade >3 . Thus, with invasive systolic PAPs (iPAPs) ≥ 50 mmHg (=isolated pulmonary hypertension [iPHT]) and echocardiographic PAPs (ePAPs) ≥ 50 mmHg (echocardiographic pulmonary hypertension [ePHT] positive), a discordant iPHT/ePHT diagnosis was considered when ePAPs differed by >10 mmHg from iPAPs. iPHT/ePHT discordance is a marker for more advanced valvular and ventricular disease and may predict the lower procedural success.¹⁹ RV–PA coupling predicts outcomes following transcatheter tricuspid intervention, but with different thresholds in women than in men.²⁰

Impaired RV–PA coupling is a major predictor of adverse outcome in patients undergoing transcatheter mitral valve replacement for severe secondary mitral regurgitation (MR) often caused by ischaemic HFrEF. The often-neglected functional and anatomical RV parameters should be systematically assessed when planning transcatheter mitral valve replacement procedures for patients with severe secondary MR.²¹

Heart Failure with Preserved Ejection Fraction

Cardiac imaging, especially echocardiography, is key to defining cardiac structure and function in HFpEF. Assessment of LV diastolic function by echocardiography is an integral part of evaluating patients with HF or symptoms of dyspnoea. In 2016, the American Society of Echocardiography and the European Association of Cardiovascular Imaging published an update on how to evaluate LV diastolic function and elevated LV filling pressures in patients with signs and symptoms of congestive HF (CHF).²² To improve diagnostic accuracy, these 2016 guidelines recommend the use of an extended algorithm including exercise E/e' , exercise tricuspid valve regurgitation velocity (TRV) and baseline e' ; to consider the exercise stress echocardiography test positive, all three criteria must be met.²²

However, a major problem with the practical application of this multimarker strategy is the inability to obtain a reliable TRV Doppler signal during exercise in 30–50% of patients, which affects the sensitivity and negative predictive value of this approach.²³ Because the positive result rate of exercise echocardiography is reported to be approximately 20%, the gold standard to obtain LV filling pressures in response to exercise remains invasive haemodynamic stress testing.²³

Diastolic HF or HFpEF is more common in elderly female patients.²⁴ Mechanisms of LV diastolic dysfunction include impaired relaxation, attenuated restoring forces and increased passive elastic stiffness that leads to elevated LV filling pressure. The presence of LV hypertrophy and dilated LA provides support for the HFpEF diagnosis.²⁵

Diastolic dysfunction is not diastolic HF, a clinical syndrome in the setting

of a normal ejection fraction. Because diastolic dysfunction is not unique to HFpEF, and is also seen in patients with HFrEF, the term 'diastolic HF' was replaced by HFpEF.²⁵

In addition, to assess diastolic function on exercise, stress echocardiography has an increasingly expanding role in the evaluation of LV systolic and chronotropic reserve, as well as other potential reasons for exercise intolerance, such as myocardial ischaemia, dynamic MR, LV outflow tract (LVOT) obstruction or an exaggerated increase in blood pressure.²⁶ Stress echocardiography is key in aortic and mitral valvular heart disease for decisions regarding the type and timing of the intervention, for determining LV contractile reserve in cardiomyopathy against the background of response to cardiac resynchronisation therapy and for determining the inducible LVOT gradient to guide therapy in hypertrophic cardiomyopathy (HCM).^{27–29}

CMR can classify diastolic dysfunction, with excellent agreement with echocardiography, using mitral inflow and myocardial tissue phase contrast analysis.³⁰ Reduced coronary microvascular density is associated with fibrosis in HFpEF.³¹ Coronary microvascular dysfunction is present in HFpEF, which limits O_2 supply relative to demand, and is associated with reserve dysfunction.³² CMR is used for the prognostication of HFpEF.³³ Mitral inflow and annular tissue Doppler velocities, as well as measurement of the LA volume index, are the most feasible and reproducible measurements.³⁴

The health of the RV at baseline is a key determinant of outcomes in HFpEF.³⁵ Impairment of RV mechanics likely starts early because of proinflammatory comorbidities, which increase myocardial stiffness: RV contractile reserve is an early marker in HFpEF.³⁶ Many clinical trial failures have led to questioning what exactly is improving, and where, and highlight the need for clinically relevant, treatment-sensitive measures with well-defined thresholds. HFpEF clinical trials should include imaging endpoints and focus more on the RV.³⁷

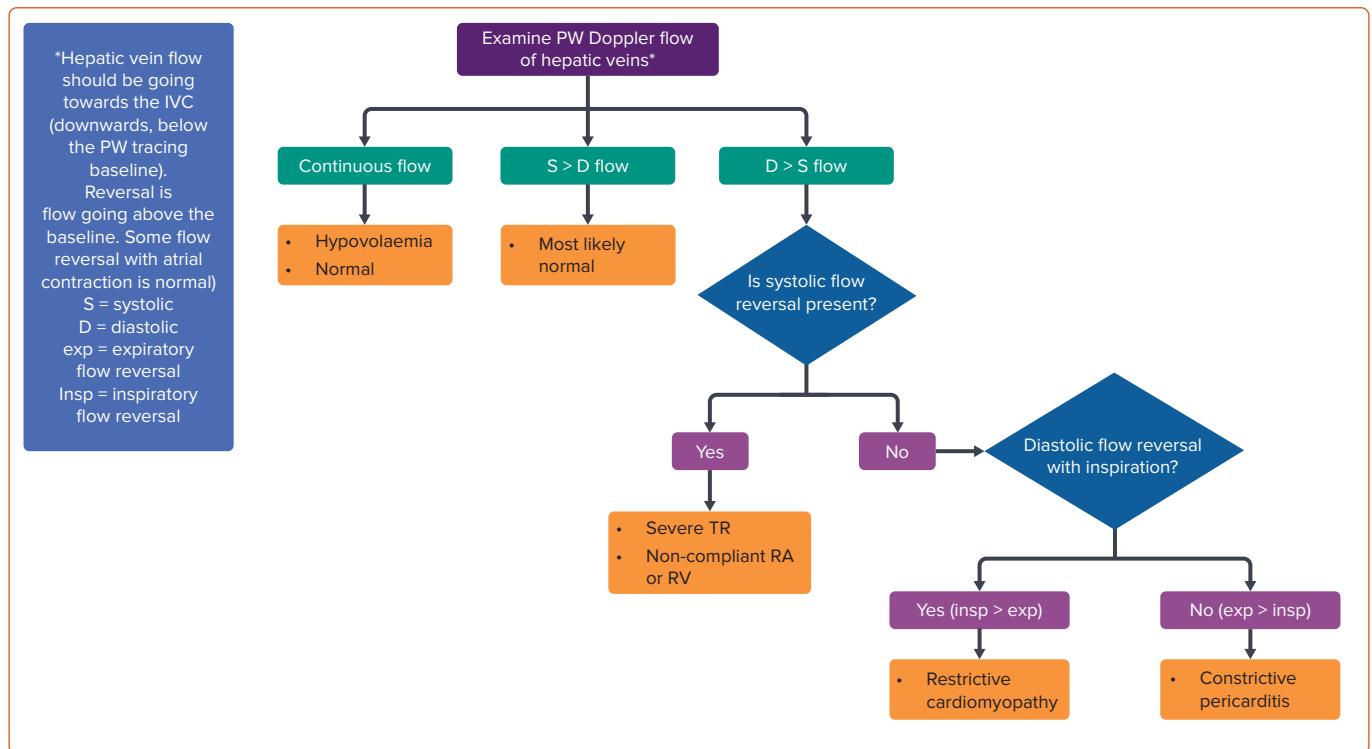
Hepatic vein imaging on echocardiography is simple and can provide insights into the underlying haemodynamic status and pathophysiology in HFpEF patients; a simple algorithm is presented in *Figure 3*.

Heart Failure with Preserved Ejection Fraction Prognostication

A meta-analysis demonstrated that CMR is an important prognostication tool for HFpEF.³³ Four cardinal features of CMR, namely the presence of a scar on late gadolinium enhancement (LGE), fibrosis on T_1 mapping, myocardial ischaemia in stress CMR and detection of RV systolic dysfunction, were identified as markers that were associated with an increased risk of major adverse cardiovascular events (MACE) and mortality in patients with HFpEF.³³ Cut-offs for LGE that showed prognostic significance ranged from 5.7% to 17% in different studies.³³ However, caution should be applied when interpreting the role of stress CMR and RV assessment in prognostication of patients with HFpEF, because the heterogeneity in this group was high in this meta-analysis due to a limited number of studies.³³ More studies are needed to assess the predictive value of these imaging parameters.

A retrospective study of more than 1,200 patients with HFpEF without known coronary artery disease (CAD) showed that both inducible ischaemia and LGE were strong independent predictors of long-term cardiovascular mortality and non-fatal MI in these populations.³⁶ Moreover, in multivariable models including conventional cardiovascular risk factors

Figure 3: Hepatic Vein Pulsed-wave Doppler Algorithm



**Hepatic vein flow should be going towards the inferior vena cava (downwards, below the PW tracing baseline). Reversal is flow going above the baseline. Some flow reversal with atrial contraction is normal. D = diastolic; exp = expiratory flow reversal; insp = inspiratory flow reversal; PW = pulsed-wave; RA = right atrium; RV = right ventricle; S = systolic; TR = tricuspid regurgitation.*

or a set of clinical covariates selected by an automated algorithm (stepwise forward Cox regression), the presence of inducible ischaemia and the extent of LGE significantly improved model discrimination in predicting MACE and the secondary composite outcome of cardiovascular mortality or hospitalisation for HF.³⁸

In addition, in a study of 110 patients with HFpEF or HFmrEF, the incidence of all-cause mortality was fivefold higher in patients who had LGE lesions (ischaemic or non-ischaemic; HR 5.3; 95% CI [1.50–18.1]; p=0.009).³⁹ This was independent of their NYHA functional class, age, gender, N-terminal pro B-type natriuretic peptide concentration, LGE mass and LVEF.³⁹

Heart Failure with Reduced Ejection Fraction

CMR can comprehensively characterise myocardial tissue and, by identifying the high-risk population, can help with a more tailored treatment of HFrEF.

In a study of 133 patients with moderate and severe LV dysfunction, the presence of LGE >6% of the myocardial volume was associated with a higher incidence of cardiovascular events, including hospitalisation, appropriate shock and all-cause mortality, in both ischaemic cardiomyopathy and non-ischaemic dilated cardiomyopathy (HR 17.8; 95% CI [8.03–39.3]; p=0.000095).⁴⁰ The incidence of cardiovascular events was significantly higher in LGE-positive patients with LVEF <30%.⁴⁰

Similarly, in a retrospective cohort of patients with HFrEF (i.e. ejection fraction between 35% and 39%), patients with both inducible ischaemia and LGE on stress CMR had an annualised rate of MACE (including cardiovascular death and non-fatal MI) of 11.7%, compared with a rate of 1.79% for patients without inducible ischaemia or infarction by LGE.⁴¹ The extent of the scar on LGE was associated with a 2.78-fold higher incidence (95% CI [1.48–4.78]; p<0.001) of the secondary outcome (a composite of

cardiovascular death or rehospitalisation), although the presence of ischaemia was not associated with the secondary outcome.⁴¹

Ischaemic Heart Disease

Among all causes of HF, ischaemic heart disease accounted for the highest proportion (26.5%) of age-standardised HF in 2017.⁴² Ischaemic HF with a mid-range or mildly reduced ejection fraction (HFmrEF) is an intermediate stage, with LVEF between 40% and 49%, that generally progresses to either HFpEF (25% of cases) or HFrEF (33% of cases).⁴³

Role of Myocardial Viability

The REVIVED BCIS2 study tested percutaneous coronary intervention (PCI) as the revascularisation modality, not coronary artery bypass grafting (CABG) as in the STICH trial, and found that PCI does not improve outcomes compared with medical therapy, even when characterised by viability status at baseline.^{44,45} Scar burden, but not viability characteristics at baseline, predicted the likelihood of LV recovery.

Although LVEF at baseline was not predictive of outcomes, scar by LGE was not only a risk stratifier, but also a predictor of early recovery for those patients with an LVEF <35%, excluding patients within a month of an acute MI. Because the inclusion criteria of the REVIVED BCIS2 study were viability, not ischaemia, one of four study patients had a low-dose dobutamine stress echocardiogram to assess for viability, whereas CMR was used in two of three study patients to assess viability by percentage transmural LGE.^{44,46}

UEAs detect the microvasculature (MV) by assessing signal intensity emanating from the myocardium as a marker of capillary blood volume. A uniform distribution of perfusion indicates a well-developed microvasculature, whereas the lack of perfusion indicates an insufficient microvasculature. Homogeneous perfusion suggests an excellent MV,

whereas the absence of perfusion suggests a lack of MV. Cardiologists should be wary of the presence of false perfusion in the thin myocardium, which, if very bright, suggests a scarred myocardium.⁴⁷

Myocardial ischaemia is known to be prognostic. The ISCHEMIA trial may have been an exception, perhaps due to collider bias, but ischaemia has no predictive utility as a therapeutic modification of risk.⁴⁸ The ISCHAEMIA trial enrolled relatively healthy older adults, with a low prevalence (23.4%) of multimorbidity (healthy selection bias), and invasive management was not associated with improved clinical outcomes in older patients.⁴⁹

Single-photon emission computed tomography (SPECT) myocardial perfusion imaging (MPI) can also evaluate myocardial viability. There are two distinct states of the myocardium: one where it is hypoperfused or dysfunctional, which can be metabolically inactive and identified as scars, and the other where it is metabolically active, indicating hibernation.⁵⁰

Approximately 50% of patients with ischaemic dysfunction of the LV have a substantial amount of dysfunction, but the myocardium is viable on SPECT.⁵¹ Long-term survival in patients with ischaemic cardiomyopathy is correlated with the amount of dysfunctional but viable myocardium, and revascularisation can improve LV function in myocardial hibernation.⁵² Zizek et al. reported that myocardial viability, which was investigated using SPECT, was independently related to the occurrence of ventricular tachycardia in patients undergoing cardiac resynchronisation therapy due to LV lead position.⁵³ Myocardial segments with decreased viability in the potential LV pacing site should be identified before the procedure to avoid possible enhancement of electrical instability.⁵³

Role of Myocardial Blood Flow

Stress PET–MPI improves the detection of severe multivessel CAD in HFrEF patients and avoids false-negative results.⁵⁴ In patients with known and suspected CAD, myocardial blood flow reserve independently predicts mortality and may help identify patients with a survival benefit after early revascularisation with PCI or CABG beyond MPI perfusion defects.⁵⁵

Myocardial Diseases

Echocardiography is the first-line imaging investigation for most forms of myocardial diseases.⁵⁶ The next step for a more accurate diagnosis is CMR, with detailed tissue characterisation revealing various infiltrating cardiomyopathies.⁵⁷

There are two main forms of fibrosis detected by CMR. CMR characterises myocardial tissue where extracellular volume (ECV) represents diffuse interstitial fibrosis, potentially reversible, and LGE represents irreversible focal fibrosis.⁵⁸

Interstitial heart disease, measured by ECV, is the final common pathway from various myocardial injuries. ECV expansion, regardless of cause, can have direct crowding effects on cardiac structure and function that lead to progressive CHF.⁵⁹

Regional replacement fibrosis is visible by LGE using a gadolinium-based contrast agent and provides precise prognostic information.⁶⁰ Diffuse interstitial fibrosis can be inferred by the T_1 mapping technique, which measures relaxation time. This technique investigates the form of focal scar or diffuse fibrosis, and may have a prognostic value for cardiac morbidity and mortality.⁶¹

Amyloid

Cardiac amyloid (CA) is caused by misfolding of one or two proteins, either a monoclonal immunoglobulin light chain (AL) or transthyretin (TTR), which is either genetically normal (wild type; ATTRwt) or due to substitution or deletion mutations (variant TTR: ATTRv).

The investigation for CA includes technetium-labelled cardiac scintigraphy (^{99m}Tc-pyrophosphate [PYP], ^{99m}Tc-3,3-diphosphono-1,2-propanodicarboxylic acid, ^{99m}Tc-hydroxymethylene diphosphonate). This easy-to-obtain nuclear bone scan using ^{99m}Tc has a high avidity to microcalcifications in TTR amyloid, but not in AL amyloid. Tracer uptake in the heart is compared to that in the rib and graded from 0 to 3 (myocardial uptake exceeds rib). The typical diagnostic threshold is >1.5. If there is Grade 2 or 3 uptake and absence of monoclonal protein (serum/urine) and typical TTE/MRI findings, there is 100% specificity for TTR cardiac amyloid.⁶²

AL amyloid can lead to Grade 1 or higher uptake: the PYP scan loses full diagnostic value for ATTR amyloid unless AL-specific laboratory testing is completely negative. AL amyloid laboratory work-up should always be sent to exclude plasma cell dyscrasia, regardless of what the PYP scan shows.⁶³ Low-intensity PYP uptake can be confused for a blood pool signal: multiplanar SPECT scans should be considered 1–2 h later to confirm that this is not a blood pool and is, instead, myocardial uptake.⁶³

Echocardiography-measured LV thickness and mass are higher in patients with ATTRwt CA, which likely reflects the longer duration of amyloid accumulation compared with AL CA or ATTRv CA.⁶⁴

In the early stages of CA, echocardiography lacks specificity to distinguish amyloid from non-amyloid infiltrative or hypertrophic heart diseases, and myocardial echogenicity described in CA is neither specific nor sensitive for amyloidosis. Decreases in LVEF tend to occur at later stages of the disease. Earlier markers of CA include relative apical sparing on strain imaging.⁶⁵ The presence of apical sparing and reduced global longitudinal strain (GLS) should raise suspicion for CA, but needs further testing with a PYP scan and laboratory work-up for AL amyloid.^{66,67} An ejection fraction to GLS ratio >4.1 may be the best echocardiographic index to diagnose CA in patients with LV hypertrophy.⁶⁸

CMR cannot reliably distinguish between AL and ATTR variants. CMR can show global subendocardial and transmural LGE, the most typical pattern, with a sensitivity of 86% and specificity of 92%.⁶⁹

Hypertrophic Cardiomyopathy

Advanced imaging allows for precise measurements of LV hypertrophy in HCM that can be confined to certain focal regions of the wall, particularly when hypertrophy is confined to the anterolateral free wall, posterior septum or apex. Along with CMR, enhanced echocardiography with UEAs also allows for the identification of additional disease features and differentiates HCM from other hypertrophic pathologies.⁷⁰

Echocardiography is generally the first imaging modality used to establish a diagnosis or exclude alternative diagnoses. Echocardiography characterises systolic anterior motion (SAM; with mitral–septal contact) with excellent temporal resolution and other mechanisms of LVOT obstruction, including muscle in the mid-cavity. MR caused by LVOT obstruction from SAM results in a jet direction that is posterior or lateral in orientation and is mostly mid-to-late systolic. Central or anterior MR jets should prompt further evaluation for intrinsic valvular or papillary abnormalities.

A diagnosis of HCM is defined as a maximum end-diastolic wall thickness ≥ 15 mm anywhere in the LV without another cause of hypertrophy. LV hypertrophy, defined here as a wall thickness of 13–14 mm, can be diagnostic when present in family members of an HCM patient or with a positive genetic test. RV hypertrophy is present in approximately 20% of patients with HCM.⁷⁰ LV morphology in HCM should be evaluated in the long-axis view. Although a sigmoid septum is the most common morphology in HCM, patients with a reverse septal curve have the greatest number of genetic mutations compared with those with a sigmoid septum.⁷¹

The challenges to obtaining an accurate wall thickness measurement vary at each level of the LV chamber. Overestimating wall thickness should be avoided by including the RV, septomarginal trabeculations and aberrant LV papillary muscles in the measurement. Other morphological abnormalities not diagnostic of HCM but part of the phenotypic expression of disease include hypertrophied and apically displaced papillary muscles, myocardial crypts, anomalous insertion of papillary muscle directly in the anterior leaflet of the mitral valve (in the absence of chordae tendineae), elongated mitral valve leaflets, myocardial bridging and RV hypertrophy.⁷² There may be incremental value to CMR over echocardiography. In one small study, echocardiography wall thickness was $\geq 10\%$ different than CMR wall thickness at diagnostic (15 mm) or prognostic (30 mm) cut-off values in 16% of patients.⁷³

To establish the presence and severity of LVOT obstruction, caution should be exercised not to contaminate the LVOT signal with MR. The MR velocity is higher, and the signal is of longer duration, spanning isovolumic contraction and relaxation, unlike the LVOT signal. The MR contour may be incomplete if the Doppler signal is not optimally aligned (*Figure 4*).

CMR has the additional benefit of producing images with contrast between the blood pool and myocardium. LGE helps estimate myocardial fibrosis as a non-invasive marker of increased risk of possible ventricular tachyarrhythmias and HF progression with systolic dysfunction.⁷⁴

The common finding in patients with HCM is coronary microvascular dysfunction, which correlates with increasing wall thickness and is associated with myocardial segmental dysfunction and interstitial fibrosis, as assessed by ECV even in segments free of LGE.⁷⁵

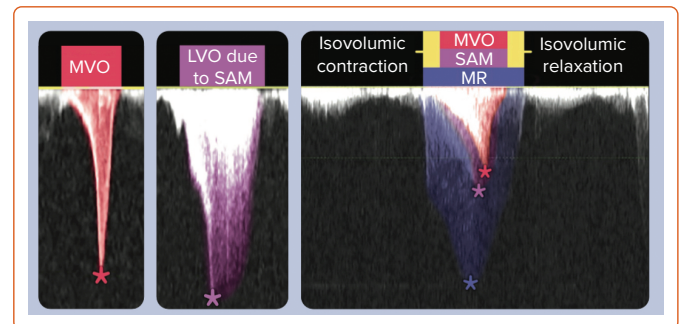
Ten per cent of HCM patients have the apical hypertrophic variant. All apical HCM patients have apical ischaemia regardless of disease severity, seen as abnormal apical perfusion defects on CMR.⁷⁶

An additional risk marker for adverse cardiovascular events that is also described in patients with HCM is an LV apical aneurysm.⁷⁷ The size of the LV aneurysm (>2 cm) and the amount of LGE in relation to global mass are key to differentiating the need for an ICD.⁷⁴ In the 2020 HCM guidelines, LV aneurysm is a second-tier risk factor that can be a nidus for non-sustained ventricular tachycardia, but there should not be a knee-jerk reaction to insert an ICD.⁷²

Currently, all HCM indications in the guidelines are based on retrospective observational data. It is difficult to predict the rare event of sudden cardiac death (SCD) in HCM, particularly in the low-risk population, which is the vast majority of HCM patients.⁷⁸

Although obstructive HCM, which accounts for two-thirds of cases, is well known, it is underappreciated that one-third of cases are non-obstructive

Figure 4: Hypertrophic Cardiomyopathy Left Ventricular Outflow Tract Versus Mitral Regurgitation Continuous-wave Doppler



HCM = hypertrophic cardiomyopathy; LVOT = left ventricular outflow tract; MR = mitral regurgitation; MVO = mid-ventricular obstruction; SAM = systolic anterior motion. Figure courtesy of Allison Hays.

HCM (nHCM) and that both carry a similar 27–30% risk of CHF.⁷¹ Myosin inhibitors for nHCM are under investigation, with the REDWOOD-HCM cohort data presented in 2023 showing the efficacy and safety of aficamten in nHCM.⁸⁰

The selection of HCM patients for septal reduction therapy relies on imaging: massive septal hypertrophy (≥ 30 mm), abnormal mitral apparatus/papillary muscles contributing to obstruction and LVOT gradient ≥ 100 mmHg at rest favour myectomy, whereas mild–moderate septal hypertrophy (ideally ≤ 18 mm) and focal colour turbulence in LVOT favour alcohol septal ablation.⁷¹

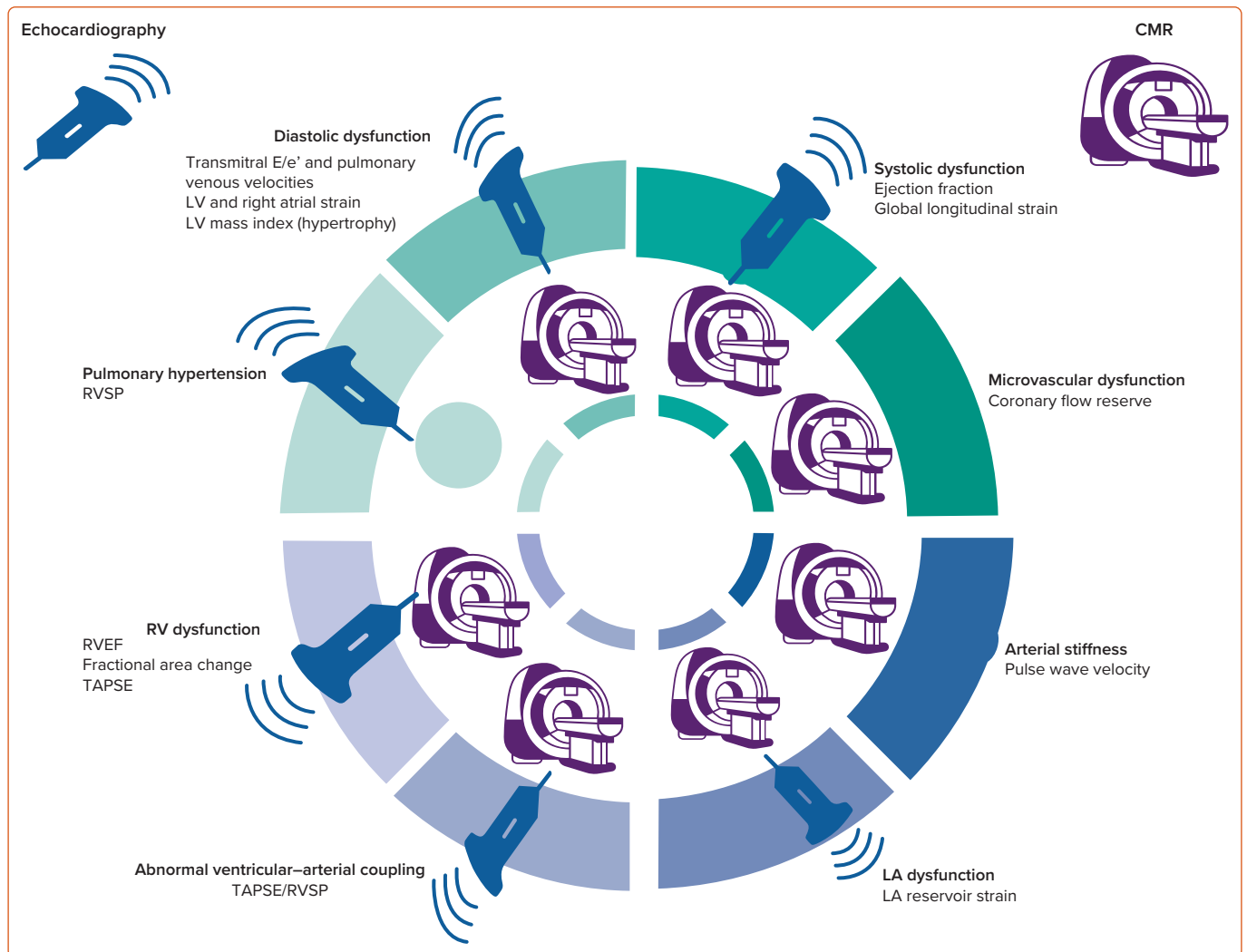
For HCM, predrug treatment with mavacamten and post-drug follow-up echocardiograms are so integral that Bristol Myers Squibb has initiated a Risk Evaluation and Mitigation Strategy (REMS) training program that must be completed before a physician is certified to administer the drug mavacamten.⁸¹ Because mavacamten initiation and treatment are guided by serial echocardiography, therapy is restricted through the REMS program, given concern for potential systolic dysfunction (i.e. LVEF $\leq 50\%$).⁸¹ Mavacamten has not been studied in patients with LVEF $< 55\%$, AF or in those who have had previous invasive septal reduction. Trials on the long-term safety and efficacy of mavacamten are ongoing. Pregnant and lactating patients were excluded from the mavacamten trials; thus, efficacy and safety in these populations remain unknown.^{82,83}

The VALOR study used core laboratory-measured LVEF, LVOT gradient at rest and Valsalva provocation, but Explorer-HCM used postexercise LVOT gradient; it remains to be seen which will be most useful in the real world.⁸⁴ Questions remain as to whether there is a role for disease modification in the preclinical stages (genotype positive/phenotype negative), as well as whether myosin inhibitors will work for nHCM or HFpEF and what their long-term safety and efficacy are.

In addition, women with HCM have a higher prevalence of pulmonary hypertension, diastolic dysfunction and smaller LV cavities, and are more likely to be a sarcomere variant carrier with less LV hypertrophy. Perhaps using sex-specific cut-off values for cardiac mass and dimensions, normalised to body size, in HCM will improve outcomes for women.⁸⁵

Stress echocardiography may be key in HCM when resting echocardiography signs associated with latent LVOT obstruction need to be evoked. When both MV coaptation length ≥ 10 mm (long) and LVOT

Figure 5: Pathophysiologies of Heart Failure



CMR = cardiac MRI; HF = heart failure; LA = left atrial; RVEF = right ventricular ejection fraction; RVSP = right ventricular systolic pressure; TAPSE = tricuspid annular plane systolic excursion.

diameter <20 mm (short) are present, severe LVOT obstruction is likely; when neither of these is seen, severe obstruction is unlikely. If either of these signs is present, further testing with CMR is needed.⁸⁶

Stress echocardiography is valuable in predicting the risk of HF (if symptomatic during stress echocardiography) in HCM patients. If an HCM patient has shortness of breath, the differential includes exercise-induced SAM, new MR or exertional arrhythmia. In these patients, proving poor diastolic function at peak stress gives an explanation of the shortness of breath and prevents unnecessary therapies, like alcohol septal ablation. Another factor for SCD in HCM is a decrease in blood pressure during an exercise stress test. Exercise stress echocardiography after a heavy meal (postprandial splanchnic vasodilation) may bring out the gradient. UEAs may mask mitral valve motion and SAM; continuous-wave Doppler across the LVOT during stress echocardiography should be used to determine E/e'.

In HCM, three of four patients have abnormal diastolic function, as measured by septal e' <7 cm/s, septal E/e' >15, LA volume index >34 ml/m² and peak TRV >2.8 m/s. Adverse outcomes (SCD, arrhythmias, CHF) increase with a score ≥3 for these four parameters, with each (i.e. septal e' <7 cm/s, septal E/e' >15, LA volume index >34 ml/m² and peak TRV >2.8 m/s) carrying 1 point.⁸⁷

The site of LGE in HCM is important, but the quantity of LGE predicts mortality.⁸⁸ LGE was defined as areas of signal intensity ≥6 SDs from normal myocardium and was expressed as the percentage of total LV myocardial mass (LGE%). Any areas that were identified as LGE by the software, but deemed artefactual on visual analysis, were manually excluded. Finally, LGE% was categorised into four risk groups (0%, 0.1–10%, 10.1–19.9%, ≥20%), each with a greater power to assess risk than just clinical scores.⁸⁸

Different phenogroups represent distinct disorders or different stages in the spectrum of disease progression, as shown in Figure 5.

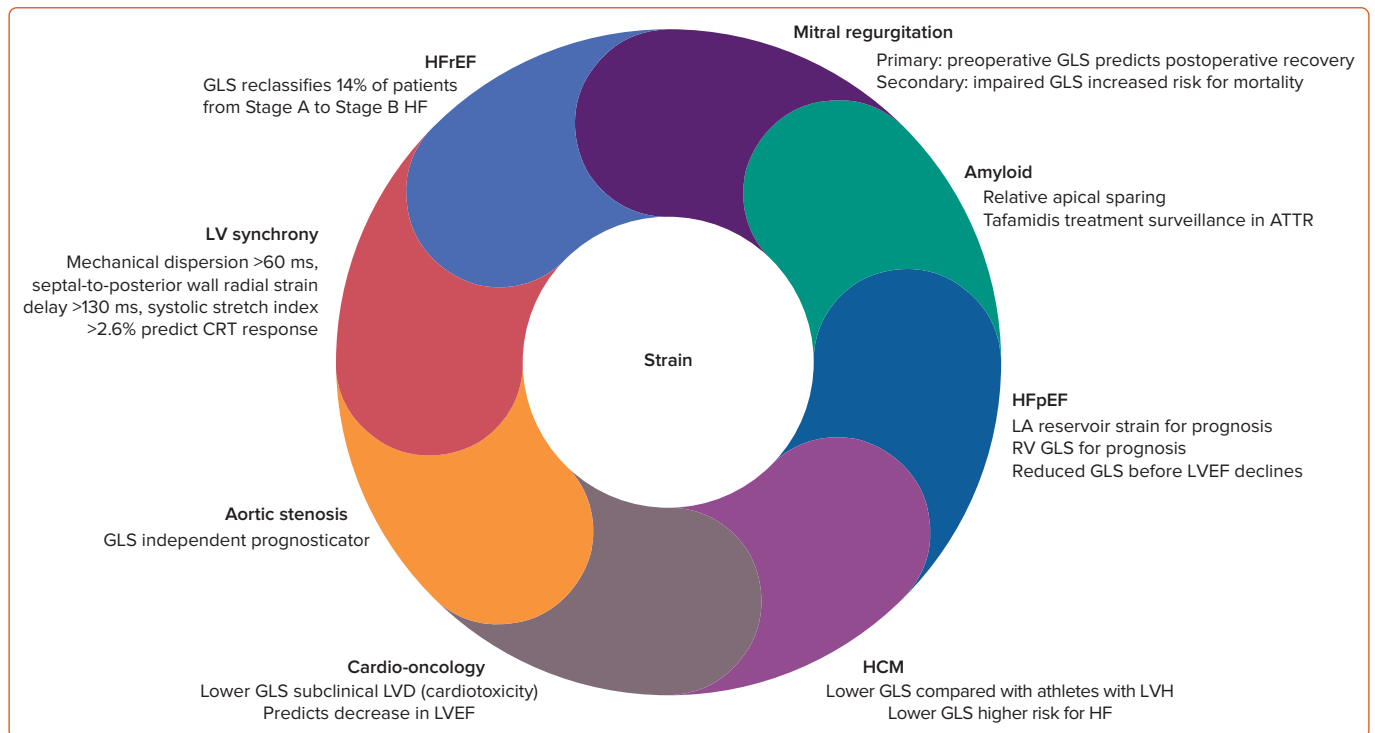
Other Cardiomyopathies

Carriers of filamin C (FLNCTv) and giant protein titin (TTNTv) truncating variants, which cause familial dilated cardiomyopathy, present with an arrhythmogenic cardiomyopathy phenotype but can be separated by CMR because FLNCTv-induced dilated cardiomyopathy has extensive myocardial fibrosis, whereas the TTNTv-induced phenotype has none or limited replacement fibrosis.⁸⁹

Strain Imaging Global Longitudinal Strain

2D speckle-tracking echocardiography (STE)-derived GLS has proven prognostic value over LVEF over a range of cardiac conditions, including

Figure 6: Global Longitudinal Strain Imaging



ATTR = transthyretin amyloidosis; GLS = global longitudinal strain; HCM = hypertrophic cardiomyopathy; HF = heart failure; HFpEF = heart failure with preserved ejection fraction; HFrEF = heart failure with reduced ejection fraction; LA = left atrium; LV = left ventricle; LVD = left ventricular dysfunction; LVEF = left ventricular ejection fraction; LVH = left ventricular hypertrophy; RV = right ventricle.

valvular, postoperative and assessment of resting LV function, especially in cardio-oncology patients.⁹⁰ Although there is variation in normal reference values according to different vendors and different software, as a general guide, a peak GLS value around -20% is normal for a healthy person and lower absolute values are considered abnormal.⁹¹ GLS has been established as an early indicator of myocardial damage in chemotherapy-induced cardiotoxicity. The stage at which LVEF decline is first detected during chemotherapy may well be too late to start HF treatment and expect full functional recovery.⁹² RV GLS is generally referred to as either RV free wall alone or an average of the septum and RV free wall segments. Peak RV free wall GLS has been demonstrated to have prognostic significance in HF.⁹³ Whereas 2D STE may be limited by geometric modelling and loss of speckles due to out-of-plane motion, 3D STE technologies have been reported to have good correlation with CMR strain measurement.⁹⁴

Image quality is paramount to optimal strain. For GLS, it is important to get the exact timing of aortic valve closure correct, avoid having the LVOT and LA in the region of interest (ROI), use a wide ROI to encompass at least 85% of the myocardium and to avoid foreshortening LV (length will determine your GLS), and image quality is key to best tracing of the ROI.

GLS should be measured routinely when HFpEF is suspected because reduced GLS is found in approximately 50–60% of patients with HFpEF.⁹⁵ Markers of elevated LV filling pressure include LA reservoir strain $<18\%$ and LA pump strain $<8\%$.⁹⁴ LA reservoir strain values vary depending on the software used to measure 2D speckle tracking.⁹⁶ Automated analysis of echocardiographic images using deep learning is more accurate in diagnosing LV systolic and diastolic dysfunction, with less variability than manual measurements performed by experts.⁹⁷

Imaging can play an even bigger role if LA strain is one of the inclusion criteria for AF trials because evidence suggests these early LA strain

markers may be additive to age over 70 years, advanced interatrial block and a $\text{CHA}_2\text{DS}_2\text{-VASc}$ score ≥ 2 to predict AF.^{92,93} Strain predicts HFpEF in nHCM, with a GLS of $<18\%$ indicating low risk for any event.⁹⁸ Relative GLS apical sparing is seen not only in amyloid cases, but also in aortic stenosis, hypertension and HCM, and can even be seen on 2D images of these patients with more robust apical thickening.⁹⁹ In sarcoidosis, the basal segments are more involved. In advanced hypertension, there is more basal scar on CMR that tracks strain.¹⁰⁰ In HCM, regional strain is awry, but regional strain has limitations.¹⁰¹ In patients with primary MR undergoing mitral valve repair, preoperative GLS can predict postoperative LVEF, whereas higher strain is observed with worsening MR and larger valves and annuli in mitral valve prolapse patients (Figure 6).^{102,103}

Future Directions

Artificial intelligence (AI) will allow HF risk assessment to be individualised, and thus allow targeted management of patients in the future.¹⁰⁴ AI can help identify various cardiac pathologies that present with the same phenotype, namely 'HFpEF', yet have different comorbidities and outcomes.¹⁰⁵ AI has identified new phenotypic clusters for SPECT MPI patients with normal visual assessments, providing improved risk stratification for all-cause mortality and major adverse events than SPECT ischaemia.¹⁰⁶ Perhaps AI could predict clots in amyloid patients.¹⁰⁷ Already, machine learning provides personalised timing of follow-up echocardiograms for patients with mild-to-moderate aortic stenosis.¹⁰⁸ Using the EchoNet algorithm, cardiologists were unable to distinguish tracings drawn by sonographers and corrected the echocardiogram readings only 1.3% of the time for AI tracings, compared with 3.1% for sonographer tracings.¹⁰⁹

Conclusion

Although ejection fraction will remain important, advanced imaging will gradually come to play a greater role in decision-making, providing

individualised risk assessment and management for patients. Specifically in the case of HFpEF, sophisticated imaging will be needed. Coordinated registries could have a role in this, with phenotyping and deep learning in patient databases adding to this knowledge base. There will be an

increasingly important role for advanced imaging and AI in the pathophysiological phenotyping of HF, especially with isolated LV diastolic dysfunction, pulmonary hypertension/RV dysfunction and LA myopathy being clarified further, ultimately improving patient outcomes. □

1. Pieske B, Tschöpe C, de Boer RA, et al. How to diagnose heart failure with preserved ejection fraction: the HFA-PEFF diagnostic algorithm: a consensus recommendation from the Heart Failure Association (HFA) of the European Society of Cardiology (ESC). *Eur Heart J* 2019;40:3297–317. <https://doi.org/10.1093/eurheartj/ehz641>; PMID: 31504452.
2. Tsao CW, Lyass A, Enserro D, et al. Temporal trends in the incidence of and mortality associated with heart failure with preserved and reduced ejection fraction. *JACC Heart Fail* 2018;6:678–85. <https://doi.org/10.1016/j.jchf.2018.03.006>; PMID: 30007560.
3. Simmonds SJ, Cuijpers I, Heymans S, Jones EAV. Cellular and molecular differences between HFpEF and HFrEF: a step ahead in an improved pathological understanding. *Cells* 2020;9:242. <https://doi.org/10.3390/cells9010242>; PMID: 31963679.
4. Bozkurt B, Coats AJS, Tsutsui H, et al. Universal definition and classification of heart failure: a report of the Heart Failure Society of America, Heart Failure Association of the European Society of Cardiology, Japanese Heart Failure Society and Writing Committee of the Universal Definition of Heart Failure: endorsed by the Canadian Heart Failure Society, Heart Failure Association of India, Cardiac Society of Australia and New Zealand, and Chinese Heart Failure Association. *Eur J Heart Fail* 2021;23:352–80. <https://doi.org/10.1002/ejhf.2115>; PMID: 33605000.
5. Shah SJ. BNP: biomarker not perfect in heart failure with preserved ejection fraction. *Eur Heart J* 2022;43:1952–4. <https://doi.org/10.1093/eurheartj/ehac121>; PMID: 35301541.
6. Reddy YNV, Kaye DM, Handoko ML, et al. Diagnosis of heart failure with preserved ejection fraction among patients with unexplained dyspnea. *JAMA Cardiol* 2022;7:891–899. <https://doi.org/10.1001/jamacardio.2022.1916>; PMID: 35830183.
7. Selvaraj S, Myhre PL, Vaduganathan M, et al. Application of diagnostic algorithms for heart failure with preserved ejection fraction to the community. *JACC Heart Fail* 2020;8:640–653. <https://doi.org/10.1016/j.jchf.2020.03.013>; PMID: 32535127.
8. Bourlaog BA, Sharma K, Shah SJ, Ho JE. Heart failure with preserved ejection fraction: JACC scientific statement. *J Am Coll Cardiol* 2023;81:1810–34. <https://doi.org/10.1016/j.jacc.2023.01.049>; PMID: 37137592.
9. Lang RM, Badano LP, Mor-Avi V, et al. Recommendations for cardiac chamber quantification by echocardiography in adults: an update from the American Society of Echocardiography and the European Association of Cardiovascular Imaging. *J Am Soc Echocardiogr* 2015;28:1–39. <https://doi.org/10.1016/j.echo.2014.10.003>; PMID: 25559473.
10. Marwick TH, Neubauer S, Petersen SE. Use of cardiac magnetic resonance and echocardiography in population-based studies: why, where, and when? *Circ Cardiovasc Imaging* 2013;6:590–6. <https://doi.org/10.1161/CIRCIMAGING.113.000498>; PMID: 23861451.
11. Guida AC, Badano LP, Ochoa-Jimenez RC, et al. Three-dimensional echocardiography to assess left ventricular geometry and function. *Expert Rev Cardiovasc Ther* 2019;17:801–15. <https://doi.org/10.1080/14779072.2019.1697234>; PMID: 31770493.
12. Dissabandara T, Lin K, Forwood M, Sun J. Validating real-time three-dimensional echocardiography against cardiac magnetic resonance, for the determination of ventricular mass, volume and ejection fraction: a meta-analysis. *Clin Res Cardiol* 2024;113:367–92. <https://doi.org/10.1007/s00392-023-02204-5>; PMID: 37079054.
13. Shimada YJ, Shiota T. A meta-analysis and investigation for the source of bias of left ventricular volumes and function by three-dimensional echocardiography in comparison with magnetic resonance imaging. *Am J Cardiol* 2011;107:126–38. <https://doi.org/10.1016/j.amjcard.2010.08.058>; PMID: 21146700.
14. Dorosz JL, Lezotte DC, Weitzenkamp DA, et al. Performance of 3-dimensional echocardiography in measuring left ventricular volumes and ejection fraction: a systematic review and meta-analysis. *J Am Coll Cardiol* 2012;59:1799–808. <https://doi.org/10.1016/j.jacc.2012.01.037>; PMID: 22575319.
15. Porter TR, Mulvagh SL, Abdelmoneim SS, et al. Clinical applications of ultrasonic enhancing agents in echocardiography: 2018 American Society of Echocardiography guidelines update. *J Am Soc Echocardiogr* 2018;31:241–74. <https://doi.org/10.1016/j.echo.2017.11.013>; PMID: 29502588.
16. Lam CSP, Roger VL, Rodeheffer RJ, et al. Pulmonary hypertension in heart failure with preserved ejection fraction: a community-based study. *J Am Coll Cardiol* 2009;53:1119–26. <https://doi.org/10.1016/j.jacc.2008.11.051>; PMID: 19324256.
17. Guazzi M, Naeije R, Arena R, et al. Echocardiography of right ventriculoarterial coupling combined with cardiopulmonary exercise testing to predict outcome in heart failure. *Chest* 2015;148:226–34. <https://doi.org/10.1378/chest.14.2065>; PMID: 25633590.
18. Bernardo RJ, Haddad F, Couture EJ, et al. Mechanics of right ventricular dysfunction in pulmonary arterial hypertension and heart failure with preserved ejection fraction. *Cardiovasc Diagn Ther* 2020;10:1580–603. <https://doi.org/10.21037/cdt-20-479>; PMID: 33224775.
19. Lurz P, Orban M, Besler C, et al. Clinical characteristics, diagnosis, and risk stratification of pulmonary hypertension in severe tricuspid regurgitation and implications for transcatheter tricuspid valve repair. *Eur Heart J* 2020;41:2785–95. <https://doi.org/10.1093/eurheartj/ehaa138>; PMID: 32176280.
20. Fortmeier V, Lachmann M, Körber MI, et al. Sex-related differences in clinical characteristics and outcome prediction among patients undergoing transcatheter tricuspid valve intervention. *JACC Cardiovasc Interv* 2023;16:909–23. <https://doi.org/10.1016/j.jcin.2023.01.378>; PMID: 37100555.
21. Karam N, Stolz L, Orban M, et al. Impact of right ventricular dysfunction on outcomes after transcatheter edge-to-edge repair for secondary mitral regurgitation. *JACC Cardiovasc Imaging* 2021;14:768–78. <https://doi.org/10.1016/j.jcmg.2020.12.015>; PMID: 33582067.
22. Nagueh SF, Smiseth OA, Appleton CP, et al. Recommendations for the evaluation of left ventricular diastolic function by echocardiography: an update from the American Society of Echocardiography and the European Association of Cardiovascular Imaging. *J Am Soc Echocardiogr* 2016;29:277–314. <https://doi.org/10.1016/j.echo.2016.01.011>; PMID: 27037982.
23. Obokata M, Kane GC, Reddy YN, et al. Role of diastolic stress testing in the evaluation for heart failure with preserved ejection fraction: a simultaneous invasive–echocardiographic study. *Circulation* 2017;135:825–38. <https://doi.org/10.1161/CIRCULATIONAHA.116.024822>; PMID: 28039229.
24. EUGenMed Cardiovascular Clinical Study Group, Regitz-Zagrosek V, Oertelt-Prigione S, et al. Gender in cardiovascular diseases: impact on clinical manifestations, management, and outcomes. *Eur Heart J* 2016;37:24–34. <https://doi.org/10.1093/eurheartj/ehv598>; PMID: 26530104.
25. Sanderson JE. Heart failure with a normal ejection fraction. *Heart (Br Card Soc)* 2007;93:155–8. <https://doi.org/10.1136/hrt.2005.074187>; PMID: 16387829.
26. Citro R, Bursi F, Bellino M, Picano E. The role of stress echocardiography in valvular heart disease. *Curr Cardiol Rep* 2022;24:1477–85. <https://doi.org/10.1007/s11886-022-01765-7>; PMID: 36040552.
27. Kosmala W, Marwick TH, Przewlocka-Kosmala M. Echocardiography in patients with heart failure: recent advances and future perspectives. *Kardiol Pol* 2021;79:5–17. <https://doi.org/10.33963/KP.15720>; PMID: 33394579.
28. Ciampi G, Carpeggiani C, Michelassi C, et al. Left ventricular contractile reserve by stress echocardiography as a predictor of response to cardiac resynchronization therapy in heart failure: a systematic review and meta-analysis. *BMC Cardiovasc Disord* 2017;17:223. <https://doi.org/10.1186/s12872-017-0657-4>; PMID: 28814264.
29. Gaitonde M, Jones S, McCracken C, et al. Evaluation of left ventricular outflow gradients during staged exercise stress echocardiography helps differentiate pediatric patients with hypertrophic cardiomyopathy from athletes and normal subjects. *Pediatr Exerc Sci* 2021;33:196–202. <https://doi.org/10.1123/pes.2020-0217>; PMID: 34303306.
30. Buss SJ, Krautz B, Schnackenburg B, et al. Classification of diastolic function with phase-contrast cardiac magnetic resonance imaging: validation with echocardiography and age-related reference values. *Clin Res Cardiol* 2014;103:441–50. <https://doi.org/10.1007/s00392-014-0669-3>; PMID: 24452509.
31. Mohammed SF, Hussain S, Mirzoyev SA, et al. Coronary microvascular rarefaction and myocardial fibrosis in heart failure with preserved ejection fraction. *Circulation* 2015;131:550–9. <https://doi.org/10.1161/CIRCULATIONAHA.114.009625>; PMID: 25552356.
32. AbouEzzeddine OF, Kemp BJ, Borlaug BA, et al. Myocardial energetics in heart failure with preserved ejection fraction. *Circ Heart Fail* 2019;12:e006240. <https://doi.org/10.1161/CIRCHEARTFAILURE.119.006240>; PMID: 31610726.
33. Assadi H, Jones R, Swift AJ, et al. Cardiac MRI for the prognostication of heart failure with preserved ejection fraction: a systematic review and meta-analysis. *Magn Reson Imaging* 2021;76:116–22. <https://doi.org/10.1016/j.mri.2020.11.011>; PMID: 33221422.
34. Chetrit M, Cremer PC, Klein AL. Imaging of diastolic dysfunction in community-based epidemiological studies and randomized controlled trials of HFpEF. *JACC Cardiovasc Imaging* 2020;13:310–26. <https://doi.org/10.1016/j.jcmg.2019.10.022>; PMID: 31918900.
35. Gorter TM, van Veldhuisen DJ, Voors AA. Rapid right-sided deterioration in heart failure with preserved ejection fraction. *Eur Heart J* 2019;40:699–702. <https://doi.org/10.1093/eurheartj/ehy900>; PMID: 30608519.
36. Singh I, Rahaghi FN, Naeije R, et al. Right ventricular–arterial uncoupling during exercise in heart failure with preserved ejection fraction: role of pulmonary vascular dysfunction. *Chest* 2019;156:933–43. <https://doi.org/10.1016/j.chest.2019.04.109>; PMID: 31103695.
37. Freed BH. REPAIRing what we can't see: the need for imaging endpoints in PAH clinical trials. *JACC Cardiovasc Imaging* 2022;15:254–6. <https://doi.org/10.1016/j.jcmg.2021.09.006>; PMID: 34801460.
38. Pezel T, Hovasse T, Sanguineti F, et al. Long-term prognostic value of stress CMR in patients with heart failure and preserved ejection fraction. *JACC Cardiovasc Imaging* 2021;14:2319–33. <https://doi.org/10.1016/j.jcmg.2021.03.010>; PMID: 34419409.
39. van Woerden G, van Veldhuisen DJ, Gorter TM, et al. The clinical and prognostic value of late gadolinium enhancement imaging in heart failure with mid-range and preserved ejection fraction. *Heart Vessels* 2022;37:273–81. <https://doi.org/10.1007/s00380-021-01910-2>; PMID: 34292389.
40. Kolluru L, Srikala J, Rao HN, et al. Incremental value of late gadolinium enhancement by cardiac MRI in risk stratification of heart failure patients with moderate and severe LV dysfunction. *Indian Heart J* 2021;73:49–55. <https://doi.org/10.1016/j.ihj.2020.11.150>; PMID: 33714409.
41. Pezel T, Sanguineti F, Kinnel M, et al. Safety and prognostic value of vasodilator stress cardiovascular magnetic resonance in patients with heart failure and reduced ejection fraction. *Circ Cardiovasc Imaging* 2020;13:e010599. <https://doi.org/10.1161/CIRCIMAGING.120.010599>; PMID: 32873071.
42. Bragazzi NL, Zhong W, Shu J, et al. Burden of heart failure and underlying causes in 195 countries and territories from 1990 to 2017. *Eur J Prev Cardiol* 2021;28:1682–90. <https://doi.org/10.1093/eurjpc/zaaa147>; PMID: 33571994.
43. Vedin O, Lam CSP, Koh AS, et al. Significance of ischemic heart disease in patients with heart failure and preserved, midrange, and reduced ejection fraction: a nationwide cohort study. *Circ Heart Fail* 2017;10:e003875. <https://doi.org/10.1161/CIRCHEARTFAILURE.117.003875>; PMID: 28615366.
44. Perera D, Ryan M, Morgan HP et al. Viability and outcomes with revascularization or medical therapy in ischemic ventricular dysfunction: a prespecified secondary analysis of the REVIVED-BICIS2 Trial. *JAMA Cardiol* 2023;8:1154–61. <https://doi.org/10.1001/jamacardio.2023.3803>; PMID: 37878295.
45. Carson P, Wertheimer J, Miller A et al. The STICH trial (Surgical Treatment for Ischemic Heart Failure): mode-of-death results. *JACC Heart Fail* 2013;1:400–8. <https://doi.org/10.1016/j.jchf.2013.04.012>; PMID: 24621972.
46. Perera D, Clayton T, O'Kane PD, et al. Percutaneous revascularization for ischemic left ventricular dysfunction. *N Engl J Med* 2022;387:1351–60. <https://doi.org/10.1056/NEJMoa2206606>; PMID: 36027563.
47. Dwivedi G, Janardhanan R, Hayat SA, et al. Prognostic value of myocardial viability detected by myocardial contrast echocardiography early after acute myocardial infarction. *J Am Coll Cardiol* 2007;50:327–34. <https://doi.org/10.1016/j.jamcollcardiol.2007.05.037>; PMID: 17431111.

- jacc.2007.03.036; PMID: 17659200.
48. Maron DJ, Hochman JS, Reynolds HR, et al. Initial invasive or conservative strategy for stable coronary disease. *N Engl J Med* 2020;382:1395–407. <https://doi.org/10.1056/NEJMoa1915922>; PMID: 32227755.
 49. Nguyen DD, Spertus JA, Alexander KP, et al. Health status and clinical outcomes in older adults with chronic coronary disease: the ISCHEMIA trial. *J Am Coll Cardiol* 2023;81:1697–709. <https://doi.org/10.1016/j.jacc.2023.02.048>; PMID: 37100486.
 50. Dorbala S, Ananthasubramanian K, Armstrong IS, et al. Single photon emission computed tomography (SPECT) myocardial perfusion imaging guidelines: instrumentation, acquisition, processing, and interpretation. *J Nucl Cardiol* 2018;25:1784–846. <https://doi.org/10.1007/s12350-018-1283-y>; PMID: 29802599.
 51. Angelidis G, Giamouzis G, Karagiannis G, et al. SPECT and PET in ischemic heart failure. *Heart Fail Rev* 2017;22:243–61. <https://doi.org/10.1007/s10741-017-9594-7>; PMID: 28150111.
 52. Page BJ, Banas MD, Suzuki G, et al. Revascularization of chronic hibernating myocardium stimulates myocyte proliferation and partially reverses chronic adaptations to ischemia. *J Am Coll Cardiol* 2015;65:684–97. <https://doi.org/10.1016/j.jacc.2014.11.040>; PMID: 25677430.
 53. Zizek D, Cvijic M, Lezaic L, Zupan I. Myocardial viability at the left ventricular lead location and the occurrence of ventricular tachyarrhythmias in cardiac resynchronization therapy. *Eur Heart J* 2013;34(Suppl 1):P1132. <https://doi.org/10.1093/eurheartj/ehz308.P1132>.
 54. Kassab K, Kattoor AJ, Doukky R. Ischemia and viability testing in new-onset heart failure. *Curr Cardiol Rep* 2020;22:76. <https://doi.org/10.1007/s11886-020-01304-2>; PMID: 32632540.
 55. Patel KK, Spertus JA, Chan PS, et al. Myocardial blood flow reserve assessed by positron emission tomography myocardial perfusion imaging identifies patients with a survival benefit from early revascularization. *Eur Heart J* 2020;41:759–68. <https://doi.org/10.1093/eurheartj/ehz389>; PMID: 31228200.
 56. Rapezzi C, Arbustini E, Caforio AL, et al. Diagnostic work-up in cardiomyopathies: bridging the gap between clinical phenotypes and final diagnosis. A position statement from the ESC Working Group on Myocardial and Pericardial Diseases. *Eur Heart J* 2013;34:1448–58. <https://doi.org/10.1093/eurheartj/ehs397>; PMID: 23211230.
 57. Argulian E, Narula J. Advanced cardiovascular imaging in clinical heart failure. *JACC Heart Fail* 2021;9:699–709. <https://doi.org/10.1016/j.jchf.2021.06.016>; PMID: 34391742.
 58. Bing R, Cavalcante JL, Everett RJ, et al. Imaging and impact of myocardial fibrosis in aortic stenosis. *JACC Cardiovasc Imaging* 2019;12:283–96. <https://doi.org/10.1016/j.jcmg.2018.11.026>; PMID: 30732723.
 59. Schelbert EB, Fonarow GC, Bonow RO, et al. Therapeutic targets in heart failure: refocusing on the myocardial interstitium. *J Am Coll Cardiol* 2014;63:2188–98. <https://doi.org/10.1016/j.jacc.2014.01.068>; PMID: 24657693.
 60. Chamshi-Pasha MA, Zhan Y, Debs D, Shah DJ. CMR in the evaluation of diastolic dysfunction and phenotyping of HFpEF: current role and future perspectives. *JACC Cardiovasc Imaging* 2020;13:283–96. <https://doi.org/10.1016/j.jcmg.2019.02.031>; PMID: 31202753.
 61. White SK, Sado DM, Fontana M, et al. T₁ mapping for myocardial extracellular volume measurement by CMR: bolus only versus primed infusion technique. *JACC Cardiovasc Imaging* 2013;6:955–62. <https://doi.org/10.1016/j.jcmg.2013.01.011>; PMID: 23582361.
 62. Gillmore JD, Maurer MS, Falk RH, et al. Nonbiopsy diagnosis of cardiac transthyretin amyloidosis. *Circulation* 2016;133:2404–12. <https://doi.org/10.1161/CIRCULATIONAHA.116.021612>; PMID: 27143678.
 63. Hanna M, Ruberg FL, Maurer MS, et al. Cardiac scintigraphy with technetium-99m-labeled bone-seeking tracers for suspected amyloidosis: JACC review topic of the week. *J Am Coll Cardiol* 2020;75:2851–62. <https://doi.org/10.1016/j.jacc.2020.04.022>; PMID: 32498813.
 64. Khor YM, Cuddy S, Falk RH, Dorbala S. Multimodality imaging in the evaluation and management of cardiac amyloidosis. *Semin Nucl Med* 2020;50:295–310. <https://doi.org/10.1053/j.semnuclmed.2020.01.001>; PMID: 32540027.
 65. Dorbala S, Cuddy S, Falk RH. How to image cardiac amyloidosis: a practical approach. *JACC Cardiovasc Imaging* 2020;13:1368–83. <https://doi.org/10.1016/j.jcmg.2019.07.015>; PMID: 31607664.
 66. Phelan D, Collier P, Thavendiranathan P, et al. Relative apical sparing of longitudinal strain using two-dimensional speckle-tracking echocardiography is both sensitive and specific for the diagnosis of cardiac amyloidosis. *Heart* 2012;98:1442–8. <https://doi.org/10.1136/heartjnl-2012-302353>; PMID: 22865865.
 67. Kyrouac D, Schiffer W, Lennep B, et al. Echocardiographic and clinical predictors of cardiac amyloidosis: limitations of apical sparing. *ESC Heart Fail* 2022;9:385–97. <https://doi.org/10.1002/ehf2.13738>; PMID: 34877800.
 68. Pagourelis ED, Mirea O, Duchenne J, et al. Echo parameters for differential diagnosis in cardiac amyloidosis: A head-to-head comparison of deformation and nondeformation parameters. *Circ Cardiovasc Imaging* 2017;10:e005588. <https://doi.org/10.1161/CIRCIMAGING.116.005588>; PMID: 28298286.
 69. Dzungu JN, Valencia O, Pinney JH, et al. CMR-based differentiation of AL and ATTR cardiac amyloidosis. *JACC Cardiovasc Imaging* 2014;7:133–42. <https://doi.org/10.1016/j.jcmg.2013.08.015>; PMID: 24412186.
 70. Maron BJ, Desai MY, Nishimura RA, et al. Diagnosis and evaluation of hypertrophic cardiomyopathy: JACC state-of-the-art review. *J Am Coll Cardiol* 2022;79:372–89. <https://doi.org/10.1016/j.jacc.2021.12.002>; PMID: 35086660.
 71. Omnen SR, Mital S, Burke MA, et al. 2020 AHA/ACC guideline for the diagnosis and treatment of patients with hypertrophic cardiomyopathy: a report of the American College of Cardiology/American Heart Association Joint Committee on Clinical Practice Guidelines. *J Am Coll Cardiol* 2020;76:e159–240. <https://doi.org/10.1016/j.jacc.2020.08.045>; PMID: 33229116.
 72. Turvey L, Augustine DX, Robinson S, et al. Transthoracic echocardiography of hypertrophic cardiomyopathy in adults: a practical guideline from the British Society of Echocardiography. *Echo Res Pract* 2021;8:G61–86. <https://doi.org/10.1530/ERP-20-0042>; PMID: 33667195.
 73. Hindieh W, Weissler-Snir A, Hammer H, et al. Discrepant measurements of maximal left ventricular wall thickness between cardiac magnetic resonance imaging and echocardiography in patients with hypertrophic cardiomyopathy. *Circ Cardiovasc Imaging* 2017;10:e006309. <https://doi.org/10.1161/CIRCIMAGING.117.006309>; PMID: 28794137.
 74. Lorenzini M, Elliott PM. Do apical aneurysms predict sudden cardiac death in hypertrophic cardiomyopathy? *Eur Heart J* 2023;44:1519–21. <https://doi.org/10.1093/eurheartj/ehad122>; PMID: 36924198.
 75. Weng Z, Yao J, Chan RH, et al. Prognostic value of LGE-CMR in HCM: a meta-analysis. *JACC Cardiovasc Imaging* 2016;9:1392–402. <https://doi.org/10.1016/j.jcmg.2016.02.031>; PMID: 27450876.
 76. Malahfid M, Senapati A, Debs D, et al. Examining the impact of inducible ischemia on myocardial fibrosis and exercise capacity in hypertrophic cardiomyopathy. *Sci Rep* 2020;10:15977. <https://doi.org/10.1038/s41598-020-71394-z>; PMID: 32994462.
 77. Hughes RK, Augusto JB, Knott K, et al. Apical ischemia is a universal feature of apical hypertrophic cardiomyopathy. *Circ Cardiovasc Imaging* 2023;16:e014907. <https://doi.org/10.1161/CIRCIMAGING.122.014907>; PMID: 36943913.
 78. Omnen SR, Ho CY, Asif IM, et al. 2024 AHA/ACC/AMSSM/HRS/PACES/SCMR guideline for the management of hypertrophic cardiomyopathy: a report of the American Heart Association/American College of Cardiology Joint Committee on Clinical Practice Guidelines. *Circulation* 2024;149:e1239–311. <https://doi.org/10.1161/CIR.0000000000001250>; PMID: 38718139.
 79. Lee DJ, Montazeri M, Bataiosu R, et al. Clinical characteristics and prognostic importance of left ventricular apical aneurysms in hypertrophic cardiomyopathy. *JACC Cardiovasc Imaging* 2022;15:1696–711. <https://doi.org/10.1016/j.jcmg.2022.03.029>; PMID: 36202449.
 80. Masri A, Sherid MV, Choudhury L, et al. Aficanten in patients with symptomatic non-obstructive hypertrophic cardiomyopathy (REDWOOD-HCM Cohort 4). *J Am Coll Cardiol* 2023;81(Suppl):609. [https://doi.org/10.1016/S0735-1097\(23\)01053-7](https://doi.org/10.1016/S0735-1097(23)01053-7).
 81. Hegde SM, Lester SJ, Solomon SD, et al. Effect of mavacamten on echocardiographic features in symptomatic patients with obstructive hypertrophic cardiomyopathy. *J Am Coll Cardiol* 2021;78:2518–32. <https://doi.org/10.1016/j.jacc.2021.09.1381>; PMID: 34915982.
 82. Bristol Myers Squibb. U.S. Food and Drug Administration approves Camzyos™ (mavacamten) for the treatment of adults with symptomatic New York Heart Association Class II–III obstructive hypertrophic cardiomyopathy (HCM) to improve functional capacity and symptoms. 28 April 2022. <https://news.bms.com/news/corporate-financial/2022/U.S.-Food-and-Drug-Administration-Approves-Camzyos-mavacamten-for-the-Treatment-of-Adults-With-Symptomatic-New-York-Heart-Association-Class-II-III-Obstructive-Hypertrophic-Cardiomyopathy-HCM-to-Improve-Functional-Capacity-and-Symptoms/default.aspx?linkid=162893103> (accessed 10 May 2023).
 83. Desai MY, Owens A, Geske JB, et al. Dose-blinded myosin inhibition in patients with obstructive hypertrophic cardiomyopathy referred for septal reduction therapy: outcomes through 32 weeks. *Circulation* 2023;147:850–863. <https://doi.org/10.1161/CIRCULATIONAHA.122.062534>; PMID: 36335531.
 84. Olivotto I, Orziak A, Barriaes-Villa R, et al. Mavacamten for treatment of symptomatic obstructive hypertrophic cardiomyopathy (EXPLORER-HCM): a randomised, double-blind, placebo-controlled, phase 3 trial. *Lancet* 2020;396:759–69. [https://doi.org/10.1016/S0140-6736\(20\)31792-X](https://doi.org/10.1016/S0140-6736(20)31792-X); PMID: 32817100.
 85. Argirò A, Ho C, Day SM, et al. Sex-related differences in genetic cardiomyopathies. *J Am Heart Assoc* 2022;11:e024947. <https://doi.org/10.1161/JAHA.121.024947>; PMID: 35470690.
 86. Jain CC, Miranda WR, Geske JB, et al. Echocardiographic characteristics of severe left ventricular outflow tract obstruction in hypertrophic cardiomyopathy. *J Am Soc Echocardiogr* 2021;34:798–801. <https://doi.org/10.1016/j.echo.2021.03.011>; PMID: 33819619.
 87. Saito C, Minami Y, Haruki S, et al. Prognostic relevance of a score for identifying diastolic dysfunction according to the 2016 American Society of Echocardiography/European Association of Cardiovascular Imaging recommendations in patients with hypertrophic cardiomyopathy. *J Am Soc Echocardiogr* 2022;35:469–76. <https://doi.org/10.1016/j.echo.2021.12.006>; PMID: 34933117.
 88. Freitas P, Ferreira AM, Arteaga-Fernández E, et al. The amount of late gadolinium enhancement outperforms current guideline-recommended criteria in the identification of patients with hypertrophic cardiomyopathy at risk of sudden cardiac death. *J Cardiovasc Magn Reson* 2019;21:50. <https://doi.org/10.1186/s12968-019-0561-4>; PMID: 31412875.
 89. Jacobs J, Van Aelst L, Breckpot J, et al. Tools to differentiate between filamin C and titin truncating variant carriers: value of MRI. *Eur J Hum Genet* 2023. <https://doi.org/10.1038/s41431-023-01357-1>; PMID: 37032351.
 90. Gherbesi E, Gianstefani S, Angeli F, et al. Myocardial strain of the left ventricle by speckle tracking echocardiography: from physics to clinical practice. *Echocardiography* 2024;41:e15753. <https://doi.org/10.1111/echo.15753>; PMID: 38284665.
 91. Mignot A, Donal E, Zaroui A, et al. Global longitudinal strain as a major predictor of cardiac events in patients with depressed left ventricular function: a multicenter study. *J Am Soc Echocardiogr* 2010;23:1019–24. <https://doi.org/10.1016/j.echo.2010.07.019>; PMID: 20810243.
 92. Lang RM, Badano LP, Mor-Avi V, et al. Recommendations for cardiac chamber quantification by echocardiography in adults: an update from the American Society of Echocardiography and the European Association of Cardiovascular Imaging. *Eur Heart J Cardiovasc Imaging* 2015;16:233–70. <https://doi.org/10.1093/ehjci/jev014>; PMID: 25712077.
 93. Liu JE, Barac A, Thavendiranathan P, Scherrer-Crosbie M. Strain imaging in cardio-oncology. *JACC CardioOncol* 2020;2:677–89. <https://doi.org/10.1016/j.jacc.2020.10.011>; PMID: 34396282.
 94. Guendouz S, Rappeneau S, Nahum J, et al. Prognostic significance and normal values of 2D strain to assess right ventricular systolic function in chronic heart failure. *Circ J* 2012;76:127–36. <https://doi.org/10.1253/circj.cj-11-0778>; PMID: 22033348.
 95. Shah AM, Claggett B, Sweitzer NK, et al. Prognostic importance of impaired systolic function in heart failure with preserved ejection fraction and the impact of spironolactone. *Circulation* 2015;133:402–14. <https://doi.org/10.1161/CIRCULATIONAHA.115.015884>; PMID: 26130119.
 96. Smiseth OA, Morris DA, Cardim N, et al. Multimodality imaging in patients with heart failure and preserved ejection fraction: an expert consensus document of the European Association of Cardiovascular Imaging. *Eur Heart J Cardiovasc Imaging* 2022;23:e34–61. <https://doi.org/10.1093/ehjci/jeab154>; PMID: 34729586.
 97. Tromp J, Seekings PJ, Hung CL, et al. Automated interpretation of systolic and diastolic function on the echocardiogram: a multicohort study. *Lancet Digit Health* 2022;4:e46–54. [https://doi.org/10.1016/S2589-7500\(21\)00235-1](https://doi.org/10.1016/S2589-7500(21)00235-1); PMID: 34863649.
 98. Hauser R, Nielsen AB, Skaarup KG, et al. Left atrial strain predicts incident atrial fibrillation in the general population: the Copenhagen City Heart Study. *Eur Heart J Cardiovasc Imaging* 2021;23:52–60. <https://doi.org/10.1093/ehjci/jeab202>; PMID: 34632488.
 99. von Roeder M, Blazek S, Rommel KP, et al. Changes in left atrial function in patients undergoing cardioversion for atrial fibrillation: relevance of left atrial strain in heart failure. *Clin Res Cardiol* 2022;11:1028–39. <https://doi.org/10.1007/s00392-021-01982-0>; PMID: 34932171.
 100. Abecasis J, Lopes P, Reis Santos R, et al. Prevalence and significance of relative apical sparing in aortic stenosis:

- insights from an echo and cardiovascular magnetic resonance study of patients referred for surgical aortic valve replacement. *Eur Heart J Cardiovasc Imaging* 2023;24:1033–42. <https://doi.org/10.1093/ehjci/jead032>; PMID: 36841934.
101. Rowin EJ, Maron BJ, Wells S, et al. Usefulness of global longitudinal strain to predict heart failure progression in patients with nonobstructive hypertrophic cardiomyopathy. *Am J Cardiol* 2021;151:86–92. <https://doi.org/10.1016/j.amjcard.2021.04.021>; PMID: 34167691.
102. Canessa M, Thamman R, Americo C, et al. Global longitudinal strain predicts survival and left ventricular function after mitral valve surgery: a meta-analysis. *Semin Thorac Cardiovasc Surg* 2021;33:337–42. <https://doi.org/10.1053/j.semtcvs.2020.09.024>; PMID: 32971244.
103. El-Tallawi KC, Zhang P, Azencott R, et al. Valve strain quantitation in normal mitral valves and mitral prolapse with variable degrees of regurgitation. *JACC Cardiovasc Imaging* 2021;14:1099–109. <https://doi.org/10.1016/j.jcmg.2021.01.006>; PMID: 33744129.
104. Muscogiuri G, Volpato V, Cau R, et al. Application of AI in cardiovascular multimodality imaging. *Heliyon* 2022;8:e10872. <https://doi.org/10.1016/j.heliyon.2022.e10872>; PMID: 36267381.
105. Segar MW, Patel KV, Ayers C, et al. Phenomapping of patients with heart failure with preserved ejection fraction using machine learning-based unsupervised cluster analysis. *Eur J Heart Fail* 2020;22:148–58. <https://doi.org/10.1002/ejhf.1621>; PMID: 31637815.
106. Bednarski B, Williams MC, Pieszko K, et al. Unsupervised machine learning improves risk stratification of patients with visual normal SPECT myocardial perfusion imaging assessments. *Eur Heart J* 2022;43(Suppl 2):ehac544.300. <https://doi.org/10.1093/eurheartj/ehac544.300>.
107. Patel R, Desai R, Sheikh MA, et al. Prevalence and risk factors associated with intracardiac thrombus in patients with cardiac amyloidosis. *J Am Coll Cardiol* 2022;79:565. [https://doi.org/10.1016/S0735-1097\(22\)01556-X](https://doi.org/10.1016/S0735-1097(22)01556-X).
108. Sánchez-Puente A, Dorado-Díaz PI, Sampredo-Gómez J, et al. Machine-learning to optimize the echocardiographic follow-up of aortic stenosis. *JACC Cardiovasc Imaging* 2023;16:733–44. <https://doi.org/10.1016/j.jcmg.2022.12.008>; PMID: 36881417.
109. He B, Kwan AC, Cho JH, et al. Blinded, randomized trial of sonographer versus AI cardiac function assessment. *Nature* 2023;616:520–4. <https://doi.org/10.1038/s41586-023-05947-3>; PMID: 37020027.